

# LOAD INTERACTION EFFECTS IN HIGH TEMPERATURE FATIGUE AND DWELL CRACK GROWTH

P. Heuler<sup>1</sup>, E. Affeldt<sup>2</sup> and R.J.H. Wanhill<sup>3</sup>

<sup>1</sup>Audi AG, Ingolstadt, Germany

<sup>2</sup>DASA AG, MTU München, Germany

<sup>3</sup>NLR, Amsterdam, The Netherlands

## ABSTRACT

High temperature fatigue in nickel-base superalloys for aero-engine applications requires consideration of cycle- and time-dependent phenomena. For waveforms with dwells and/or low frequencies crack growth rates may be significantly accelerated up to the point of fully time-dependent crack growth. In the paper, the interaction of fatigue (cycle-dependent) and dwell (time-dependent) crack growth is addressed using a broad database for IN 718 tested at 600°C. Waveforms with dwells at as well as below maximum load levels are applied to standard CT and CC specimens and blunt notched specimens. It is demonstrated that both the level of dwells with respect to the maximum load level within a cycle as well as the specific conditions at the notch root considerably affect the significance of dwells for fatigue crack growth.

## INTRODUCTION

The design of aero-engines aims at increased efficiency in terms of higher thrust-to-weight ratios and/or longer operational lives. Both the introduction of advanced materials as well as extending the limits of existing materials with regard to stress and temperature levels are being considered. Thus the classical low cycle fatigue properties of materials used in safety critical components have to be examined for temperature regimes where time-dependent phenomena become active. Lifting procedures increasingly extend the classical "crack initiation" based concepts by consideration of fatigue crack growth. Characterisation of crack growth rates and fracture modes as well as development and qualification of robust predictive models represent key elements of this process.

High temperature time-dependent crack growth in nickel-base superalloys is known to be controlled by a number of variables including stress intensity, load ratio, temperature, frequency and hold or dwell times where a limited interdependence between these variables is assumed [1]. The frequency and dwell effects are often presented via so-called mechanism maps [2-4] which indicate increased growth rates for waveforms with low frequency and/or dwell periods at high - typically max - stress levels. Commonly three regimes can be separated where crack growth appears to be either (a) fully cycle-dependent, (b) fully time-dependent or (c) mixed time/cycle-dependent. Usually the corresponding fracture modes are (a) fully or predominantly transgranular, (b) intergranular or (c) mixed trans- and intergranular. Time dependency predominantly is environmentally-controlled rather than by creep.

In the following, results are reported obtained from a collaborative research programme on lifting procedures for critical aero-engine components [5]. The present paper focuses on factors which influence the

interaction of time- and cycle-dependent fatigue such as load sequence and geometric features introducing stress concentrations in Inconel 718 at 600°C.

## MATERIAL AND TEST DETAILS

The material was a batch of 440 mm diameter x 66 mm thick forged pancakes of IN 718 with a heat-treatment well-established to obtain optimum creep resistance consisting of annealing at 955°C/1h, air cool, ageing at 720°C/8h, furnace cool to 620°C, 620°C/8h, air cool. The resulting mechanical properties at 600°C were  $R_{p0.2} = 1030$  MPa,  $R_m = 1230$  MPa and elongation = 17 %. The grain size was ASTM 8 or finer, i.e. nominal grain diameter = 22  $\mu$ m.

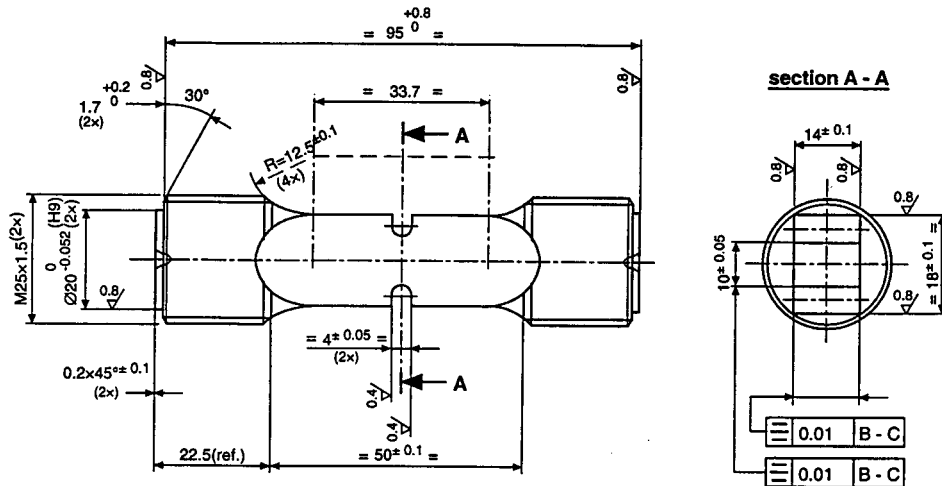


**Figure 1:** Double edge notched specimen with notch radius 2 mm

Compact-tension (CT) specimens with  $w = 26$  mm and  $b = 13$  mm and corner crack (CC) specimens of 8x8 mm cross section were used to characterise the material behaviour under baseline and complex loading environments. A double edge notched specimen design, Fig. 1, was used to introduce a stress concentration feature with  $K_t = 2.23$ . The notches were machined by one of two processes adopting (a) a drilling and grinding route in order to minimise residual stresses or (b) broaching which is a common route to produce fir tree fixtures in the rim area of aero-engine discs. Notched specimens were tested either with a 0.2 mm corner slit as crack starter or without any artificial crack starters where one or several cracks mainly in the centre area of the notches freely initiated. These cracks are designated as "surface" cracks in this paper. Here crack "initiation" and growth was monitored through careful post-test SEM fracture surface evaluation of striations and of beach marks left behind by high R ratio marker load blocks [6,7]. Crack growth from corner slits was monitored via a long range high magnification optical microscope as well as DC PD measurements [8]. Stress-strain and strain-life data were obtained from LCF specimens of 8 mm diameter and 28 mm gauge length.

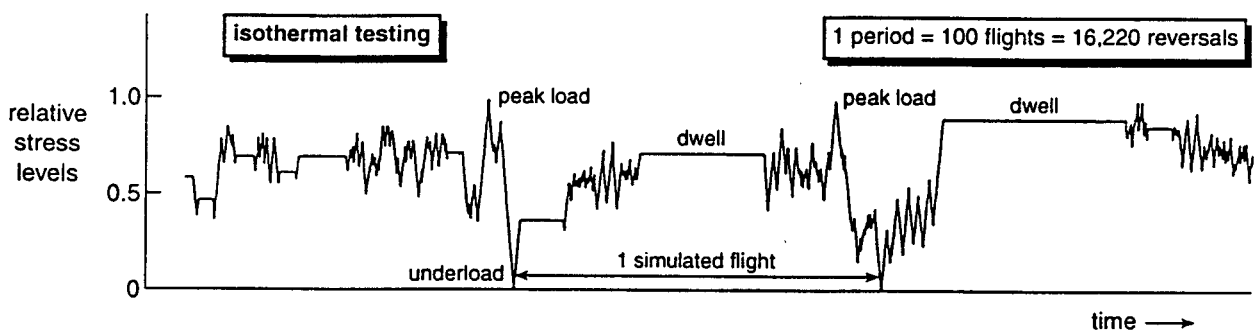


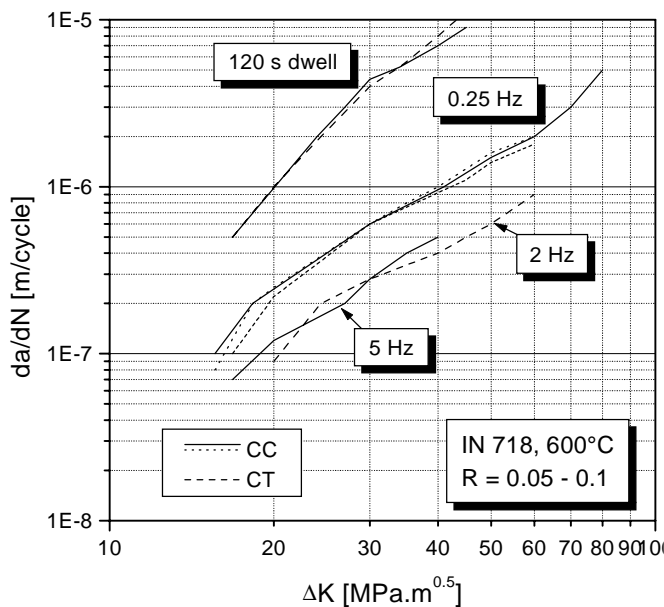
**Figure 2:** Representative section of the standardised load sequence Hot TURBISTAN

The waveforms adopted were sinusoidal with 2 Hz and trapezoidal with 1 s ramps and 1 s dwell times at max and min level, respectively. The latter waveform is - in this paper - designated as 0.25 Hz. Cyclic dwell tests included 120 s hold times at max as well as at intermediate levels of about 80 % of max. For the latter, the dwell periods were interspersed either before or after the maximum load reversal. The test programme also considered the standardised load history Hot TURBISTAN [9], Fig. 2, which had been derived as an (isothermalised) load or rpm sequence representative for the rim area of hot section rotating components where dwells at max rpm levels occur rather infrequently. It consists of 100 flights of different lengths including 689 dwell periods with a maximum single dwell time of about 800 s and a total accumulated dwell time of 8 hours per 100 flights.

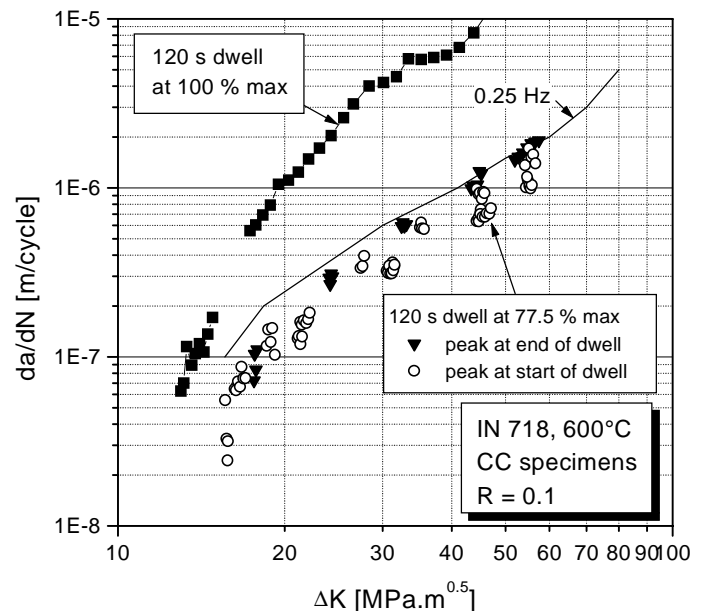
## EFFECTS OF PEAK LOADS ON FATIGUE AND DWELL CRACK GROWTH

Fig. 3 shows the effect of cycle frequency and dwell periods on crack rates as determined from CC and CT specimens tested under low R ratios. As is well-known the dwell periods at max stress levels significantly accelerate growth rates by more than an order of magnitude. It is the common view that grain boundary embrittlement and fracture induced by oxygen or water vapour controls that process. This is supported by high vacuum test data showing a fully cycle-dependent behaviour with transgranular cracking with a faceted fracture surface appearance or striations [10]. The growth rates of Fig. 3 compare well with literature data [3] indicating fully time-dependent crack growth for 120 s dwell at max which can actually be predicted from dwell crack growth data for sustained loading [11].

When dwell periods are included at intermediate levels of about 80 % of max stress level, the dwell effect is drastically reduced or totally absent, Fig. 4. In order to limit test duration, the tests of Fig. 4 were conducted sequentially adopting 120 s dwell cycling interrupted by 0.25 Hz cycling. The dwells were interspersed within the descending or ascending load branch designated by "peak before dwell" or "peak after dwell", respectively. Since the "peak" load occurs in every cycle, it is applied for  $\Delta S$  and  $\Delta K$  calculations; it must not be interpreted as an overload known, for example, from airframe applications.



**Fig. 3:** Effect of waveform and frequency on crack growth rates



**Fig. 4:** Effect of position of dwell load level relative to the maximum load level of the cycle

Since there is a distinct  $K_{max}$  dependence of dwell crack growth, the overall stress level of one of the "peak" load tests was adjusted such that the stress level for the dwell periods at 77.5 % was identical to the

100 % stress level in the tests with dwells at max. In spite of this, the dwell effect was again not visible in the "peak" load test. The results of Fig. 4 are very much in line with data presented in [12] where it was demonstrated that dwells at intermediate levels (50 and 75 % of max) essentially did not accelerate crack growth rates under pure 1 Hz cycling.

Comparison of predicted versus actual crack growth rates for CC specimens tested under the Hot TURBISTAN load sequence gives further evidence to the limited or suppressed effect of dwell periods which do not occur at max stress levels. Crack growth lives between about 2200 and 4200 flights were successfully predicted (or even underestimated by a factor of 1.5) based on 0.25 Hz data without any (further) consideration of hold time contributions. Note that the total accumulated dwell times were between 170 and 330 hours in these tests.

### ***Fractographic Observations***

Microstructural observations made in the present study confirm previous findings indicating a predominantly intergranular cracking mechanism with increased growth rates for high R ratios and/or dwell periods at max stress level. Fig. 5 gives a series of macrographs showing crack tunneling and ragged crack fronts of CC specimens tested under 120s dwell at max, Figs. 5a and 5b. However a predominantly transgranular fracture mode is found in a specimen (Fig.5c) where four sections of 120 s dwell at 77.5 % of max have repeatedly been applied within 0.25 Hz cycling. For low  $\Delta K$  levels up to the second section with dwells,  $K_{max}$  during the dwell period was below the threshold for the onset of dwell cracking of about  $17 \text{ MPa} \sqrt{\text{m}}$  at  $600^\circ\text{C}$  [11]. During the third and fourth sections with dwells the main crack grew transgranularly, but a trend towards intergranular cracking with increasing crack lengths was observed. Therefore a transient behaviour may have been present.



**Figure 5:** Macrographs of CC specimens tested under (a) 120 s dwell, R=0.1, (b) 120 s dwell, R=0.5, (c) 4 sections of 120 s dwell at 77.5 % of max + 0.25 Hz, R=0.1

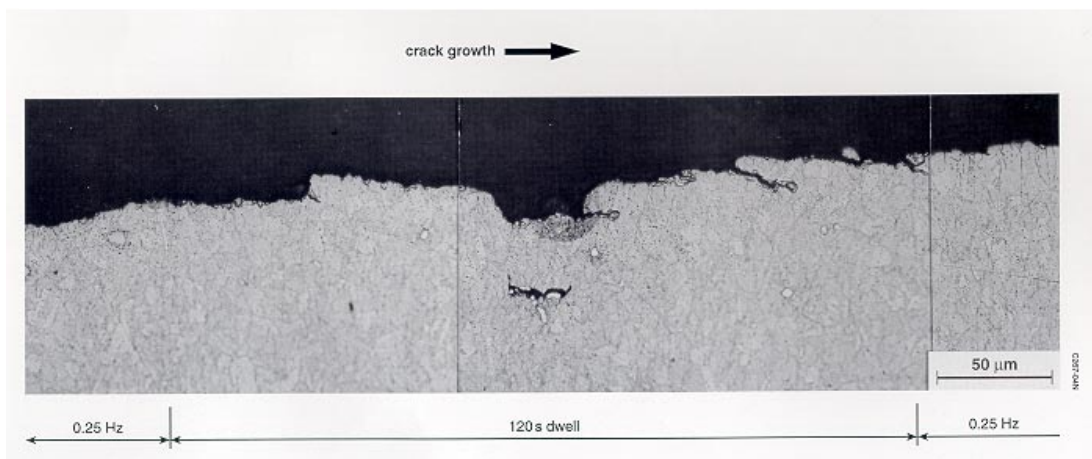


**Figure 6:** Crack path in the fourth section of 120 s dwell at 77.5 % of max showing secondary cracking and crack branching

More important, however, is the occurrence of secondary or branched dwell cracking, Fig. 6. Crack branching lowers the actual crack tip stress intensity, i.e. the crack driving force. It is concluded that for cycles with dwells below max the enhancement of secondary cracking is at least one of the major sources for the suppression of dwell-cracking-induced acceleration of growth rates. Since it has been observed that sequences with "peaks" after dwells lead to slightly higher growth rates than those with "peaks" before dwells, the residual stress state ahead of the crack tip may also influence the crack driving force.

## CRACK GROWTH FROM BLUNT NOTCHES

Crack growth data for corner and surface cracks of double notched specimens are given in Figs. 7 to 9. The  $\Delta K$  values are calculated in a straight-forward manner using a specific solution developed in [13] based on the Newman-Raju formulae assuming linear elastic conditions. The effect of notch root plasticity is addressed below. The data of Figs. 7 and 8 exhibit a considerable degree of scatter which may be due to the different routes of machining, but also due to the different procedures to monitor crack growth. Moreover, these data have been generated by several test laboratories.

Fig. 7 shows the expected effect of waveform with regard to 2 Hz and 0.25 Hz cycling. The most striking result, however, is the apparent missing effect of the 120 s dwell period. In particular at lower  $\Delta K$  levels growth rates are equal to or even lower than for the 0.25 Hz signal. Fig. 8 presents the data for cycling with 120 s dwell at max or at 80 % of max, respectively. Within the range of scatter, the "peak" loads do not retard the growth rates as has been shown for the CC specimens, Fig. 4. This is, of course, due to the fact that the growth rates for dwells at max load are already very similar to those for 0.25 Hz. The "peak" loads do not introduce further retardation below this level.

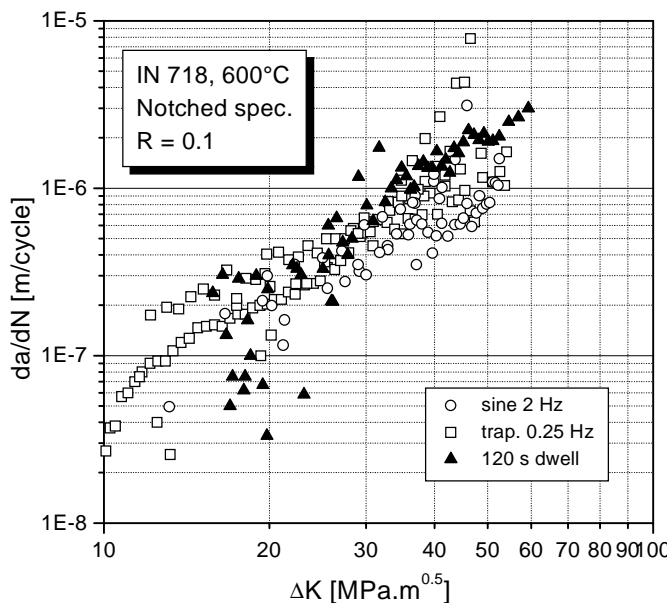


**Fig. 7:** Effects of waveform and frequency on crack growth from notches (surface and corner cracks)

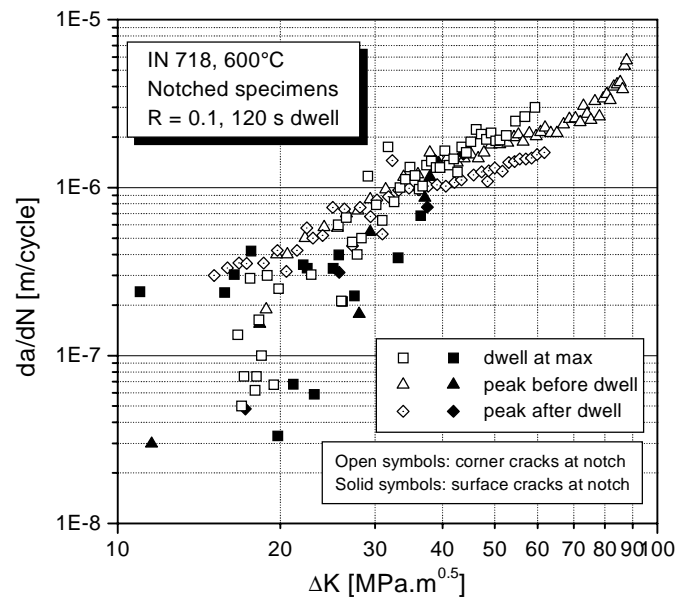


**Fig. 8:** Effect of dwell load level (100 and 80 %) relative to the maximum load level of the cycle

### Fractographic Observations

Fracture surfaces of the notched specimens showed intergranular or mixed inter-/transgranular cracking modes. At small crack length under loading waveforms with dwells at max and/or high R ratios intergranular crack growth dominated, although fatigue striations could also be identified which were severely oxidised in most cases. It is interesting to note that in the notched specimens at small crack sizes, intergranular cracking which appears to be indicative of dwell cracking did not promote accelerated crack

growth. In some cases a transition to a transgranular cracking mode was visible close to final fracture. This finding can possibly be related to the growth rate gradually exceeding the diffusion rate of oxygen along grain boundaries.

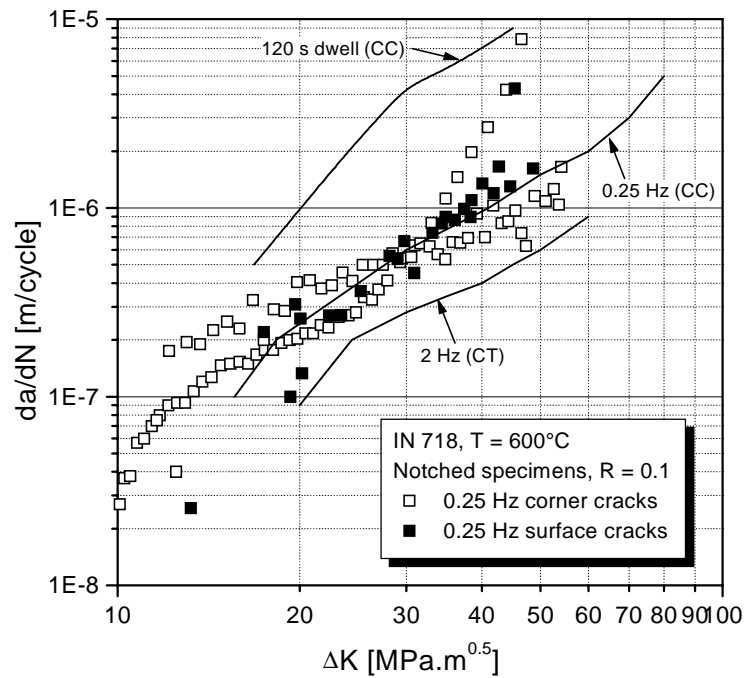


**Fig. 9:** Comparison of crack growth data from standard C and CT specimens and double edge notched specimens

## DISCUSSION

The assessment of fatigue strength and in-service life during the design stage generally requires the transfer of a set of material data to critical locations of the component under consideration. In Fig. 9 the base-line crack growth data from CC and CT specimens of Fig. 3 are superimposed on the notched specimen crack growth data for the 0.25 Hz waveform (1 s dwell at max and min) at  $R = 0.1$ . On average the material data apparently describe the notched specimen data quite well. A closer look, however, reveals distinct differences between the stress-strain states of the CC/CT specimens and the material in the notch stress field, in particular for small crack lengths prevailing for the majority of fatigue life. The CC specimens were tested with max stress levels of 550 and 600 MPa, i.e. in the nominally elastic domain, whereas the notched specimen maximum net section stress levels were between 600 and 800 MPa (up to 900 MPa for extreme cases). These load levels produce extensive monotonic plastic deformation in the notch area with plastic zone sizes between about 0.5 and 1.5 mm. Upon unloading, the local stress goes into compression leading to negative  $R$  ratios for external  $R = 0.1$  loading. This is illustrated in Fig. 10 where the development of local  $R$  ratios for the first 30 cycles are plotted in the vicinity of the notch root area based on a complex Chaboche-type stress-strain modelling within a FE model of the notched specimen [14]. A simplified prediction using the local strain concept adopting stabilised cyclic stress-strain data leads to similar estimates, Table 1.

The apparent fit of the  $R = 0.1$  material data with the behaviour of cracks growing from the notch root in Fig. 9 must be viewed as fortuitous since up to about  $\Delta K = 50 \text{ MPa}\sqrt{\text{m}}$  the crack depth is below 1 mm and thus well within the notch monotonic plastic zone. Table 1 indicates even some **cyclic** plastic deformation in the immediate notch root area which would invalidate a linear-elastic  $K$  concept. Obviously the reduced  $R$  ratios at the notch - which would reduce the effective crack tip driving force - and the cyclic plasticity -

which would increase the crack tip driving force - counterbalance each other producing a net result as given in Fig. 9. For smooth specimens under strain control, Rosenberger and Ghonem [15] have demonstrated a successful description of crack growth under cyclic inelastic conditions using based both strain-based and J based equivalent stress intensity concepts.

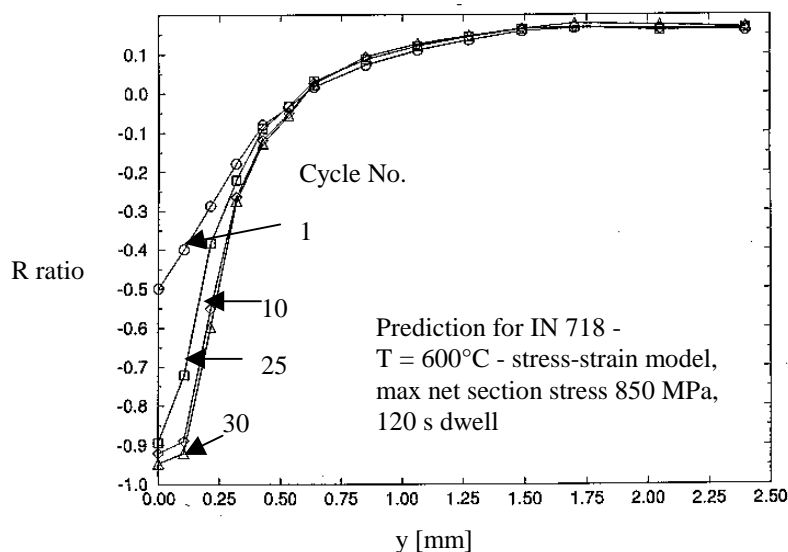


**Figure 10:** Local R ratio in the notch root ( $y = 0$ ) and the interior ( $y > 0$ ) of the double edge notched specimen as predicted for the first 30 cycles by FE adopting a Chaboche-type stress-strain model [14]

TABLE 1  
LOCAL STRESS-STRAIN IN THE NOTCH ROOT PREDICTED BY THE LOCAL STRAIN CONCEPT

$S_{\max}$ [MPa]	$\sigma_{\max}$ [MPa]	$R_{\sigma}$	$\Delta\varepsilon$ [%]	$\Delta\varepsilon_{el}$ [%]	$\Delta\varepsilon_{pl}$ [%]
600	813	-0.40	0.72	0.68	0.041
700	852	-0.48	0.85	0.76	0.095
800	887	-0.53	0.99	0.81	0.176
900	920	-0.56	1.14	0.86	0.281

The monotonic plastic deformation in the notch root area upon initial loading plays a prominent role also for explaining the reduced effect for dwell periods even at max load. In [16,17] it has been shown that prestraining promotes high slip densities and a more homogeneous plastic deformation which in turn hinders (or suppresses) the oxidation-controlled dwell cracking process.

The interaction phenomenon of "peak" loads on dwell crack growth, i.e. the reduction or suppression of the detrimental effect of dwell periods during sustained or cycling loading, will certainly be influenced by the local stress states at the crack tip. This phenomenon is, however, not yet fully understood and needs further investigation. In [12] it has been proposed to take account of dwell periods only for those occurring at max stress levels by a linear superposition of fatigue- and dwell-(time-)dependent crack growth contributions. However, application to real-life loading environments is needed to verify or reject this type of approach.

## CONCLUDING REMARKS

Lifing of critical engine components made of nickel-base superalloys generally requires consideration of a "crack initiation" phase in order to demonstrate economic design margins. If advanced fracture mechanics based concepts are to be applied to extend the usable life span or to replace (part of) the classical lifing concept based on LCF data, crack growth has to be examined for small crack sizes which typically would

represent freely nucleated cracks under the influence of the local stress-strain fields at stress concentration features. Then crack growth under these conditions needs to be addressed for both an appropriate interpretation of experimental findings and transfer to realistic lifing procedures. With regard to the findings discussed in the paper, the clarification and substantiation of the phenomena appears attractive since it may help to avoid overly conservative design procedures.

## Acknowledgements

The helpful discussions with the working group members of the collaborative research programme reported in [5] with representatives from IABG, MTU, RWTH, NLR, EGT and DERA are gratefully acknowledged. Specimen manufacturing (broaching of notches) was supported by EGT (now ABB Alstom Power), Lincoln, UK.

## REFERENCES

1. Tong, J. and Byrne, J. (1999), *Fatigue Fract Engng Mater Struct* **22**, 185.
2. Solomon, H.D. (1973), *Metall Trans*, 341.
3. Weerasooriya, T. (1988) In: *Fracture Mechanics: Nineteenth Symposium*, pp. 907-923. Cruse, T.A. (Ed.), ASTM, Philadelphia, USA.
4. Nicholas, T. and Ashbaugh, N.E. (1988) In: *Fracture Mechanics: Nineteenth Symposium*, pp. 800-817. Cruse, T.A. (Ed.), ASTM, Philadelphia, USA.
5. Heuler, P. and Bergmann, J.W. (1997), Report No. B-TA-3602, IABG, Ottobrunn, Germany.
6. Wanhill, R.J.H., Hattenberg, T. and ten Hoeve, H.J. (1996), Report No. CR 96451 C, NLR, Amsterdam, The Netherlands.
7. Affeldt, E. (1996), Report No. N96ELB-0012, MTU, München, Germany.
8. Boogers, J.A.M. and Wanhill, R.J.H. (1995), Report No. CR 95058 L, NLR, Amsterdam, The Netherlands.
9. Bergmann, J.W. and Schütz, W. (1990), Report No. TF-2809, IABG, Ottobrunn, Germany.
10. Bache, M.R., Evans, W.J. and Hardy, M.C. (1999), *Int J Fatigue* **21**, S69.
11. Wanhill, R.J.H. and Boogers, J.A.M. (1993), Report No. TP 93300 L, NLR, Amsterdam, The Netherlands.
12. Nicholas, T. and Weerasooriya, T. (1986) In: *Fracture Mechanics: Seventeenth Volume*, pp. 155-168, ASTM, Philadelphia, USA.
13. Herbel, M., Amstutz, H., Dankert, M. and Seeger, T. (1993), Report No. FI-111/1993, Technical University Darmstadt, Germany.
14. Höschler, K. (1999), PhD Thesis, RWTH Aachen, Germany.
15. Rosenberger, A.H. and Ghonem, H. (1992), *Fatigue Fract Engng Mater Struct* **15**, 1125.
16. Zheng, D., Rosenberger, A.H. and Ghonem, H. (1992), *Materials Sci Engng* **A161**, 13.
17. Ghonem, H., Nicholas, T. and Pineau, A. (1993), *Fatigue Fract Engng Mater Struct* **16**, 577.